ARTICLE

Hierarchic Self-Assembly of Nanoporous Chiral Networks with Conformationally Flexible Porphyrins

David Écija,[†,*] Knud Seufert,[†] Daniel Heim,[†] Willi Auwärter,[†,*] Claudia Aurisicchio,[‡] Chiara Fabbro,[§] Davide Bonifazi,[‡,§,*] and Johannes V. Barth[†]

[†]Physik Department E20, Technische Universität München, D-85748 Garching, Germany, [‡]Department of Chemistry, University of Namur, Rue de Bruxelles 61, B-5000 Namur, Belgium, and [§]Department of Pharmaceutical Sciences, University of Trieste, Piazzale Europa 1, I-34127 Trieste, Italy

ABSTRACT We report the hierarchic design of homochiral 2D nanoporous networks under ultrahigh vacuum conditions on the Ag(111) surface by using a flexible porphyrin derivative as a primary unit. The conformational adaptation of the molecular module gives rise to two enantiomers upon 2D confinement, which self-assemble in enantiopure clusters made of three molecules reflecting chiral recognition, which constitute the secondary supramolecular building block mediating the formation of the tertiary complex open networks. Our results show that the creation of homochiral superstructures based on the hierarchical assembly of conformationally flexible molecular components constitutes a unique pathway toward the design of novel and functional chiral structures.

KEYWORDS: chirality · hierarchic self-assembly · STM · porphyrins · nanochemistry

The improved control of molecular self-assembly is of paramount importance for the development of functional nanostructured materials.[1] In particular, pathways are sought to mimic the ubiquitous multilevel structural design of natural systems. In recent years, assembly protocols were introduced to tailor distinct hierarchic architectures using well-defined surfaces as construction platforms, where molecular-level observations are possible using scanning tunneling microscopy (STM).[2−12] In many cases, the surface confinement leads to a simultaneous expression of interesting chirality phenomena, notably organizational chirality with achiral, prochiral, or chiral molecular species.[13,14] Consequently, hierarchical molecular assembly has also attracted increasing interest for the engineering of multilevel ordered low-dimensional chiral aggregates or networks.

Flexible molecular building blocks have already been exploited toward the design of simple 2D porous layers.[15−17] However, very little attention has been paid to the role of the chiral induction that originates from the conformational adaptation of adsorbed molecules giving rise to the formation of surface enantiomers,[18−21] which effect was recently designated as "conformational chirality".[22] In particular, appealing systems to study are those based on porphyrins, as they could yield novel catalytic properties or energy conversion reaction centers.[23−26]

Herein we report an STM study of the hierarchic design of homochiral 2D nanoporous networks under ultrahigh vacuum conditions on the Ag(111) surface by using a flexible porphyrin derivative as a primary unit. The conformational adaptation of the molecular module gives rise to two enantiomers upon 2D confinement, which self-assemble in extended homochiral patterns. In this process, we identify an enantiopure cluster made of three molecules reflecting chiral recognition, which constitutes the secondary supramolecular building block mediating the formation of the tertiary complex open networks.

RESULTS AND DISCUSSION

Porphyrin derivative **1** is based on a tetrapyrrolic core differently substituted at the four *meso*-positions, presenting two phen-1,4-diylethynylpyridyl (PhC≡CPyr) and two 3,5-di-*tert*-butyl (*t*-Bu$_2$Ph) substituents at the 5,15 and 10,20 *meso*-positions, respectively (*cf.* Figure 1a).[20,21] A key characteristic of this porphyrin module is its inherent conformational flexibility resulting in a conformational adaptation upon adsorption on a surface, in agreement with earlier observations using simpler porphyrin species.[27−34] Specifically, all *meso*-substituents can rotate around the macrocycle−phenyl axis, often inducing a nonplanar deformation of the tetrapyrrolic core. In addition, the ability to rotate the peripheral *tert*-butyl (*t*-Bu) fragments can in-

*Address correspondence to david.ecija.fernandez@ph.tum.de, wilhelm.auwaerter@ph.tum.de, davide.bonifazi@fundp.ac.be.

Received for review June 14, 2010 and accepted July 16, 2010.

Published online July 29, 2010. 10.1021/nn1013337

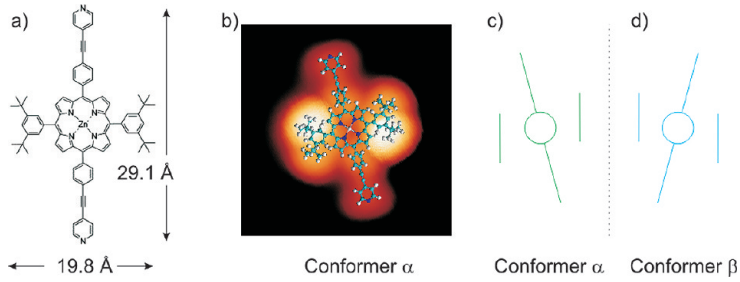

Figure 1. (a) Scheme of compound 1; (b) STM image (3.8 × 3.8 nm^2, I = 0.05 nA, U_t = 2 V) of an isolated molecule adsorbed on Ag(111) with an overlaid model to identify the different subunits; (c,d) cartoon representation of conformers α and β.

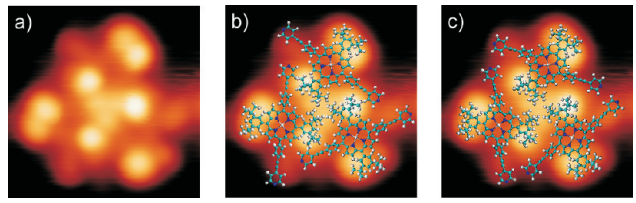

Figure 2. Supramolecular trimer reflecting the chiroselective assembly of compound 1 surface conformers on Ag(111): (a) STM image of the three-molecule seed; (b,c) superposition of the straight-leg and the bent-leg model in panel a, revealing a flexure of the PhC≡CPyr legs (image size = 4.67 × 4.67 nm^2, I = 0.2 nA, U_t = 1 V).

duce peculiar contrast and symmetry variations in STM images.[20,21] Accordingly, molecular mechanics simulations showed that the PhC≡CPyr legs are quite flexible; that is, the orientation of the *meso*-PhC≡CPyr leg and the porphyrin core can deviate from the straight equilibrium position toward the *t*-Bu_2Ph substituents.[21]

The deposition of a small concentration of **1** on Ag(111) held at 350 K results in the decoration of the step edges and the formation of small molecular aggregates and some isolated molecules, which were investigated by STM following cool down to temperatures <10 K. Figure 1b shows an image with intramolecular resolution for an isolated species, in nice agreement with our previous experiments on Ag(111) and Cu(111), where coordination complexes were studied.[20,21] Upon adsorption, module **1** deconvolutes into two chiral conformers, labeled as α and β, as a consequence of their conformational flexibility, which plays a major role in the formation of enantiopure porous domains (*vide infra*). Because of the inherent nonchirality of the gas-phase molecule, there is an equal probability for each enantiomer to be found on the surface. The surface chiral conformational adaptation of module **1** results in an angle of ±15° between the molecular board and the axis connecting the two lobes (*i.e.*, the *t*-Bu_2Ph moieties; Figure 1c,d);[20,21] however, the PhC≡CPyr legs are oriented in a straight fashion for isolated species.

Figure 2a shows the secondary trimeric molecular aggregate. This noncovalent assembly, called α-I, is identified as the seed of the tertiary extended supramolecular pattern described below. Each of the three bright double-lobed features in the corners of the assembly corresponds to one *t*-Bu_2Ph moiety. Furthermore, the protrusions originating from the PhC≡CPyr substituents are discernible. If we assign each *t*-Bu_2Ph moiety to one molecule and superpose a structural model from Figure 1b on the STM image, aligning the *t*-Bu_2Ph legs with the close-packed directions of the substrate, we obtain three different molecular orientations in the trimeric seed: following the substrate symmetry, the modules are rotated by 0, 60, and 120° relative to each other (Figure 2b). The *t*-Bu_2Ph groups in the model correctly represent the two-lobe structures visible in the STM data. However, the positions of the PhC≡CPyr substituents deviate from the protrusions in the STM image, as clearly seen for the three outer PhC≡CPyr groups in Figure 2b. Thus, the structural model, which perfectly describes an individual module, does not fit the molecular structure in the trimeric assembly. To achieve structural agreement for the seed and for the extended pattern (*vide infra*), we have to introduce a bending of ~20° of the PhC≡CPyr moieties (*cf.* Figure 2c). This distortion is a consequence from the

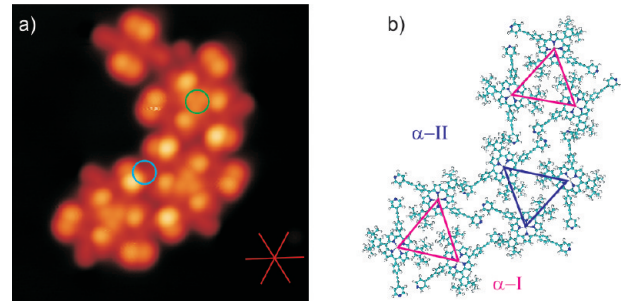

Figure 3. Combination of secondary structural units. (a) STM image of three trimeric seeds with deviations from isolated trimer characteristics marked. The red star represents the close-packed directions of Ag(111). (b) Tentative model displaying the molecular arrangement in image a. Seed α-I is marked by a magenta triangular contour, whereas seed α-II is outlined in purple. Colored circles emphasize intermolecular interactions (see text) (image size = 11.07 × 11.07 nm^2, I = 0.2 nA, U_t = −1 V).

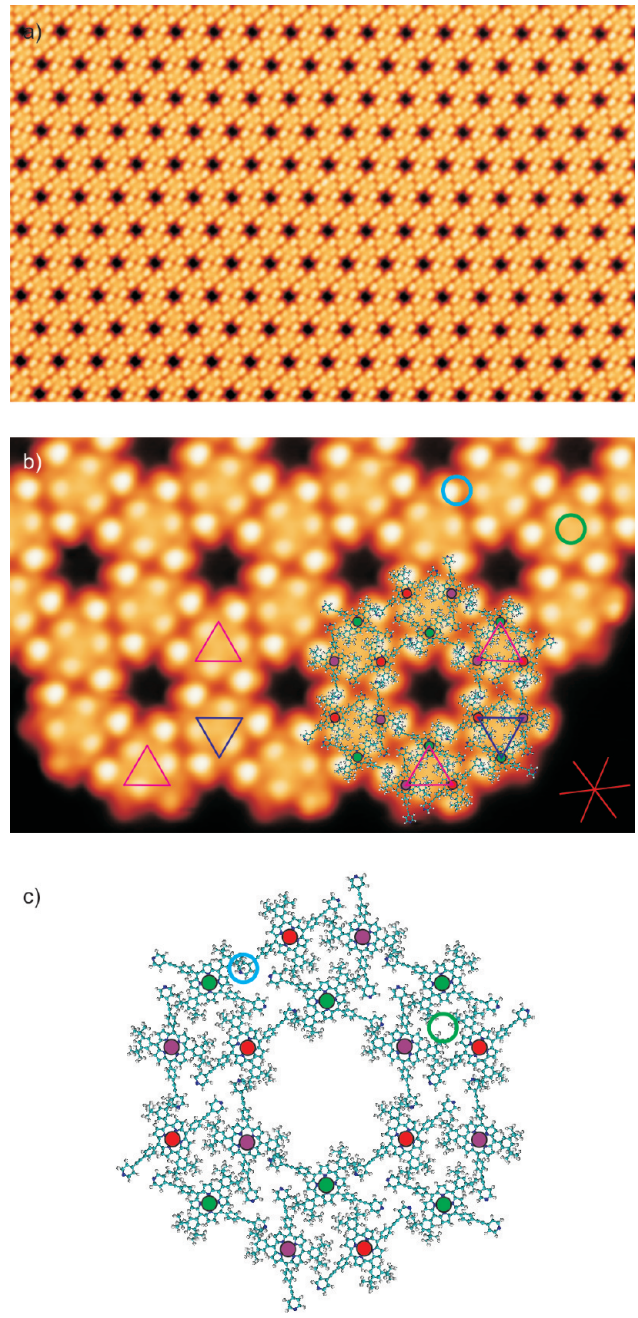

Figure 4. Extended homochiral domains with multilevel order. (a) STM overview image (88.10 × 56.01 nm^2, I = 0.2 nA, U_t = 1 V). (b) close-up (23.33 × 14.81 nm^2, I = 0.2 nA, U_t = 1 V) with superposition of model assembly containing distorted porphyrin modules. In order to distinguish the orientation of the molecule with respect to the substrate (red, 0°; green, 60°; purple, 120°), different colored circles are depicted on top of the Zn(II) metal centers of the porphyrins. (c) Molecular pattern surrounding a single pore. Circular colored lines are used to outline the intermolecular interactions (see text). Magenta and purple triangles depict supramolecular units α-I and α-II, respectively. The red star indicates all dense-packed substrate directions.

intermolecular steric hindrance between the PhC≡CPyr and the *t*-Bu$_2$Ph substituents in the supramolecular assemblies. Importantly, the trimer is an enantiopure arrangement consisting exclusively of the same conformers; that is, its assembly implies a chiral recognition process.[35]

The three-molecule seed represents a secondary supramolecular unit with two distinct surface orientations (α-I and α-II; *cf.* Figure 3) related by a 60° rotation, reflecting the symmetry of the fcc surface. The combined assembly of these supramolecular units to a larger aggregate is illustrated by the STM data in Figure 3a. Comparing the STM images of a trimeric seed (Figure 2a) with the larger assembly shown, one notices the appearance of additional brighter protrusions within the latter structure. These bright protrusions originate from the close proximity of the PhC≡CPyr and *t*-Bu groups (*cf.* Figure 3b and *vide in-*

fra). As the imaging characteristics appear independent of bias voltage conditions, we relate them to the molecular topography, that is, a rotation of the *t*-Bu and pyridyl moieties minimizing steric hindrance. In fact, the lock-in mechanism that bonds the α-I and α-II seeds is based on the van der Waals and weak hydrogen-bonding interactions between the PhC≡CPyr moieties and the *t*-Bu groups, as depicted in Figure 3 (blue circle).

At higher coverages, extended domains of a highly regular hexagonal supramolecular porous network are created by the alternation of units α-I and α-II (Figure 4). The interporous distance is 54 ± 3 Å, whereas the unit cell vectors of the supramolecular pattern form an angle of −11 ± 5° with respect to the close-packed directions of Ag(111). Within the experimental error, the pattern is commensurate with the substrate.

Regarding the intermolecular forces, the pores are stabilized by (see circles in Figures 3a and 4b,c) (a) van der Waals and weak hydrogen-bonding interactions between the PhC≡CPyr substituent and the adjacent *t*-Bu_2Ph (blue circle) moiety; (b) van der Waals interaction between the *t*-Bu_2Phs groups,[19,28] involving three molecules (green circle). As a result, each molecule is connected to four neighbors, and all reactive pyridyl end groups are engaged in noncovalent bonding for the porous network structure.

Both mirror-symmetric chiral domains of the hexagonal porous architectures have been observed: α-networks (*cf.* Figures 2, 3, 4, 5a,b,e) and β-networks (Figure 5c,d,f) made of conformers α and β, respectively. Figure 6 shows the coexistence of both enantiopure domains in the very same image. The unit cell vectors of the network made by the β conformers form an angle of 11° with respect to the close-packed directions of the substrate. Thus the transition from the single enantiomer on the surface to the porous chiral domain implies three levels of hierarchy, where strictly the same enantiomers are involved, outlining a chirality transfer: conformer → seed → porous network (*cf.* Figure 5).

The high mobility of the molecular modules combined with the reported chiral recognition yields exceptionally large homochiral domains, often resulting in only one homochiral domain per terrace (*cf.* Figure 6). The selection of one chirality might be triggered by the random aggregation of three isomers into a trimeric seed as shown above. We discard any conformational adaptation of a conformer arriving at the border of a homochiral island made of the opposite conformer since we visualized both conformers at the boundaries of the domains and any manipulation with the STM tip in order to mirror the conformer at the boundary was unsuccessful.[36] Furthermore, some islands are strictly found on a terrace without any border connected to the steps, which seems to suggest that chiral surface defects like kinks are not playing a major role as the starting point for the formation of the chiral supramolecular pattern.

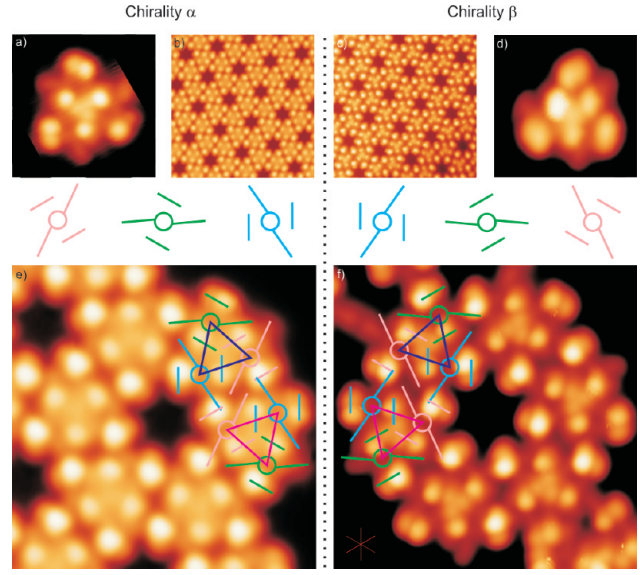

Figure 5. Mirror-symmetric homochiral networks from conformational surface enantiomers showing the transfer of homochirality. (a,b,e) α-Chirality signature; (c,d,f) β-chirality signature with respective trimeric seeds and porous domains. Each domain is composed of strictly one enantiomer. For clarity, the three possible molecular orientations for each conformer are depicted in light pink, green, and blue colors, respectively. The red star indicates all dense-packed substrate directions. Seeds α-I (β-I) and α-II (β-II) are depicted by a magenta and a purple triangle, respectively. The dotted line represents the mirror plane. Tunneling parameters: (a,e) I = 0.2 nA, U_t = 1 V; (b−d,f) I = 0.2 nA, U_t = −1 V. Images size: (a,d) 5.5 × 5.5 nm²; (b,c) 22.5 × 22.5 nm²; (e,f) 10.1 × 10.1 nm².

Concerning applications, the size of the pore amounts to ≈3 nm², which can be exploited to selectively accommodate molecular guest species. This feature is particularly interesting for functional electron acceptor molecules that could yield an interesting optically active reaction center together with the electronically donating porphyrin molecules. An example for a pore hosting an individual porphyrin guest is shown in Figure 7. The symmetry of the pore allows for three different azimuthal orientations of the porphyrin guest: its PhC≡CPyr legs lock in to the indentations along the inner rim of the pore. In addition, the guest porphyrin is not exactly located in the center of the pore, but slightly dis-

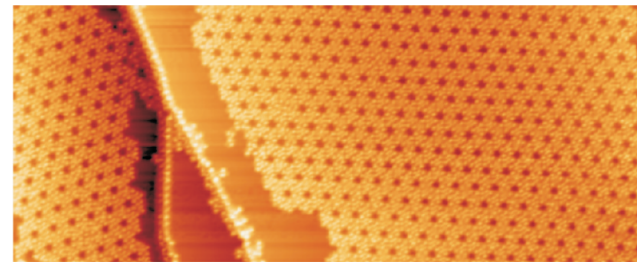

Figure 6. Formation of homochiral domains in adjacent terraces after the adsorption of compound 1 on Ag(111). The high mobility of the molecular modules combined with the chiral recognition induces exceptionally large homochiral domains, often resulting in the creation of only one homochiral domain per terrace. Image size: 169.7 × 69.4 nm². Tunneling parameters: I = 0.2 nA, U_t = −1 V.

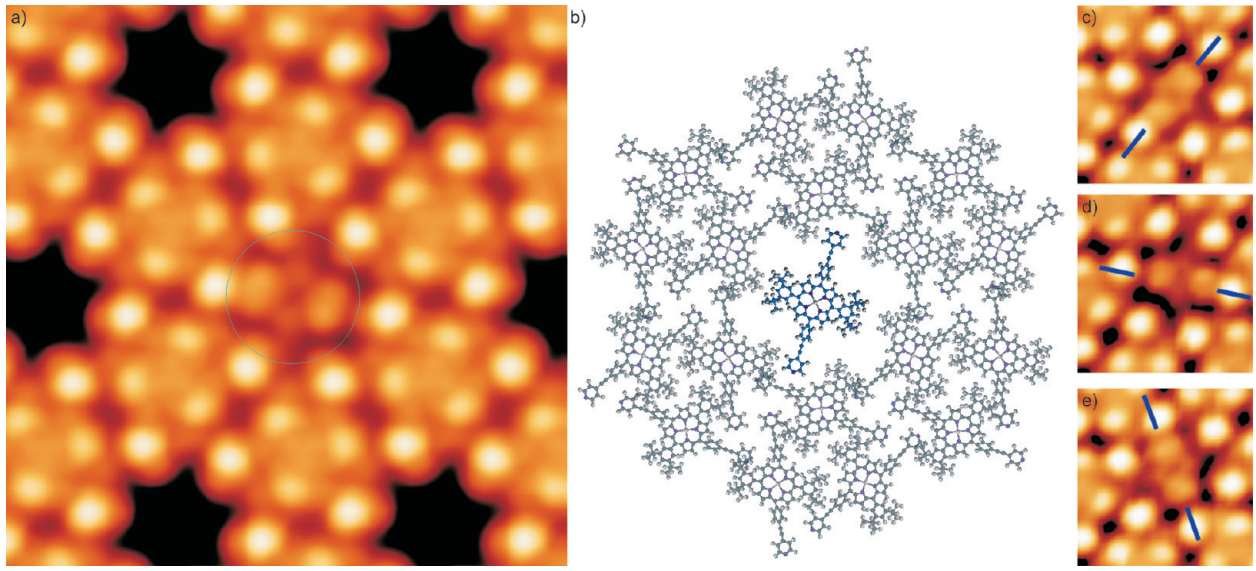

Figure 7. Host−guest interaction in the nanoporous network formed after the adsorption of compound 1 on Ag(111). (a) Central pore accommodates an additional porphyrin module (outlined by a blue circle) due to the sieving properties of the supramolecular pattern. Image size: 11.1 × 11.1 nm^2. Tunnel parameters: I = 0.2 nA, U_t = 1 V. (b) Schematic model displaying the nonsymmetric placement of the guest molecule within the pore in panel a. (c−e) Three different azimuthal orientations of a guest within the pore (marked by blue lines). Tunneling parameters: I = 0.2 nA, U_t = −1 V.

placed. This asymmetry suggests that the lateral position of the guest is mainly determined by the van der Waals interaction between one *t*-Bu_2Ph group of the guest and one *t*-Bu_2Ph group of a neighboring molecule from the supramolecular host pattern, which favors an offset toward either side of the pore (*cf.* Figure 7b). Consequently, the porphyrin can be locked in six different configurations. In this sense, Figure 7a,c,d,e nicely reflects four possible configurations observed in the same enantiopure domain.

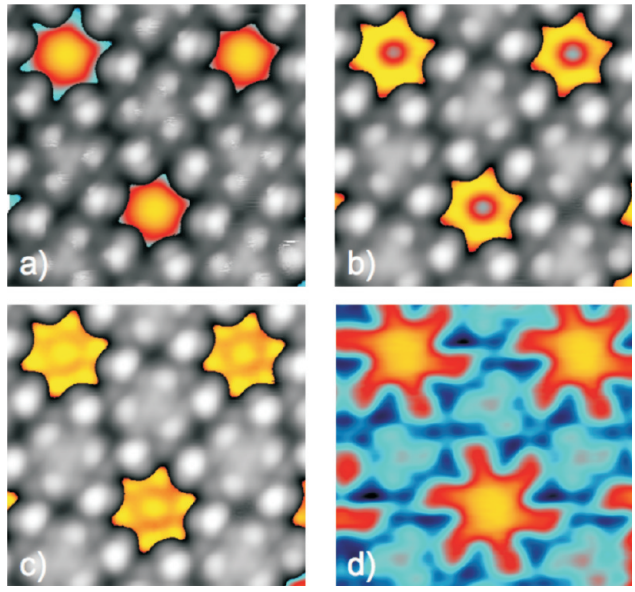

Figure 8. (a−c) Confinement of Ag(111) surface state electrons within the pores of the hierarchic porphyrin network. The d*I*/d*U* maps presented in color are superimposed on topographic STM images (grayscale). (a−c) Series of bias voltages (a, 100 mV; b, 450 mV; c, 750 mV) representing standing wave patterns of increasing complexity. In this bias range, the topographic image does not change drastically. The d*I*/d*U* map reproduced in panel d and taken at a voltage of 2.5 V nicely shows that the chiral nature of the supramolecular network is directly reflected in the electronic charge density distribution of this system.

Furthermore, Figure 8 demonstrates the modification of the Ag(111) surface electronic structure by the porphyrin network. Recent reports highlight the potential of highly regular supramolecular gratings and networks to tune the electronic properties at the interface.[37,39] Specifically, the pores might act as coupled quantum dots,[38] and the Ag(111) surface state electrons can experience quantum confinement effects, which in turn guide the positioning of guest species.[39,40] Indeed Figure 8a−c shows standing wave patterns of progressive complexity for a series of increasing bias voltages, representing electron confinement in the pores. In addition, the chiral nature of the supramolecular assembly is directly reflected in the corresponding charge density distributions (*cf.* Figure 8d). Consequently, this 2D chiral network represents a model system to explore potentially novel phenomena in chiral molecular hosting, paving new ways to understand enantioselectivity.

CONCLUSIONS

In summary, we have described the formation of extended and highly regular homochiral nanoporous networks on a smooth metal substrate, through a three-level hierarchical chiral self-assembly process, which is based on a flexible porphyrin derivative adopting a chiral conformation upon surface confinement. We suggest that the engineering of homochiral superstructures based on the hierarchical assembly of conformationally flex-

ible molecular components constitutes a unique pathway toward the design of novel and functional chiral structures. In addition, the porosity of the networks might be useful for patterning and guest accommodation,[41−48] including chiroselective molecular recognition and quantum well formation. This strategy could be extended to other important molecular building blocks, opening new avenues toward novel and potentially adaptive complex functional materials.

METHODS

All STM experiments were performed in a custom-designed ultrahigh vacuum (UHV) system providing a base pressure below 1×10^{-10} mbar.[49] The monocrystalline Ag(111) substrate was cleaned by repeated Ar^+ sputtering cycles at an energy of 800 eV, followed by annealing at 730 K for 10 min. Subsequently, a submonolayer coverage of porphyrin derivative **1** was deposited by organic molecular beam epitaxy from a thoroughly degassed quartz crucible held at 700 K. During deposition, the Ag(111) surface was kept at 343 K and the pressure remained $<5 \times 10^{-10}$ mbar. All data were acquired employing a low-temperature CreaTec-STM[50] with the sample held at 6 K using electrochemically etched W tips. In the figure captions, U_t refers to the bias voltage applied to the sample. Simulations were performed in the framework of the Hyperchem 7.5 software package.[51] The WSxM software was used for the analysis of STM images.[52]

Acknowledgment. Work was supported by the ESF project FunSmarts and the Munich Center for Advanced Photonics (MAP). D.B. especially acknowledges the University of Namur, the Belgian National Research Foundation (FRS-FNRS, through Contract Nos. 2.4.625.08F and F.4.505.10.F), the "Loterie Nationale", and the Région Wallonne through the "SOLWATT" program (Contract No. 850551), the "TINTIN" ARC project from the Belgian French Community (Contract No. 09/14-023). D.E. thanks the European Commission for support through the Marie Curie IntraEuropean Fellowship for Career Development FP7 program (Project Nanolanta, Proposal No. 235722).

REFERENCES AND NOTES

1. Ariga, K.; Hill, J. P.; Lee, M. V.; Vinu, A.; Charvet, R.; Acharya, S. Challenges and Breakthroughs in Recent Research on Self-Assembly. *Sci. Technol. Adv. Mater.* **2008**, *9*, 14109.
2. Spillmann, H.; Dmitriev, A.; Lin, N.; Messina, P.; Barth, J. V.; Kern, K. Hierarchical Assembly of Two-Dimensional Homochiral Nanocavity Arrays. *J. Am. Chem. Soc.* **2003**, *125*, 10725–10728.
3. Barlow, S. M.; Louafi, S.; Le Roux, D.; Williams, J.; Muryn, C.; Haq, S.; Raval, R. Supramolecular Assembly of Strongly Chemisorbed Size- and Shape-Defined Chiral Clusters: S- and R-Alanine on Cu(110). *Langmuir* **2004**, *20*, 7171–7176.
4. Blüm, M.-C.; Cavar, E.; Pivetta, M.; Patthey, F.; Schneider, W.-D. Conservation of Chirality in a Hierarchical Supramolecular Self-Assembled Structure with Pentagonal Symmetry. *Angew. Chem., Int. Ed.* **2005**, *44*, 5334–5337.
5. Clair, S.; Pons, S.; Brune, H.; Kern, K.; Barth, J. V. Mesoscopic Metallosupramolecular Texturing by Hierarchic Assembly. *Angew. Chem., Int. Ed.* **2005**, *44*, 7294–7297.
6. Barth, J. V. Molecular Architectonic on Metal Surfaces. *Annu. Rev. Phys. Chem.* **2007**, *58*, 375–407.
7. Bléger, D.; Kreher, D.; Mathevet, F.; Attias, A. J.; Schull, G.; Huard, A.; Douillard, L.; Fiorini-Debuischert, C.; Charra, F. Hierarchically Self-Assembled Host−Guest Network at the Solid−Liquid Interface for Single-Molecule Manipulation. *Angew. Chem., Int. Ed.* **2007**, *46*, 7404–7407.
8. Katano, S.; Kim, Y.; Matsubara, H.; Kitagawa, T.; Kawai, M. Hierarchical Chiral Framework Based on a Rigid Adamantane Tripod on Au(111). *J. Am. Chem. Soc.* **2007**, *129*, 2511–2515.
9. Staniec, P. A.; Perdigão, L. M. A.; Saywell, A.; Champness, N. R.; Beton, P. H. Hierarchical Organisation on a Two-Dimensional Supramolecular Network. *ChemPhysChem* **2007**, *8*, 2177–2181.
10. Lei, S.; Surin, M.; Tahara, K.; Adisoejoso, J.; Lazzaroni, R.; Tobe, Y.; Feyter, S. D. Programmable Hierarchical Three-Component 2D Assembly at a Liquid−Solid Interface: Recognition, Selection, and Transformation. *Nano Lett.* **2008**, *8*, 2541–2546.
11. Schlickum, U.; Decker, R.; Klappenberger, F.; Zoppellaro, G.; Klyatskaya, S.; Auwärter, W.; Neppl, S.; Kern, K.; Brune, H.; Ruben, M.; Barth, J. V. Chiral Kagome Lattice from Simple Ditopic Molecular Bricks. *J. Am. Chem. Soc.* **2008**, *130*, 11778–11782.
12. Yang, Y.; Wang, C. Hierarchical Construction of Self-Assembled Low-Dimensional Molecular Architectures Observed by Using Scanning Tunneling Microscopy. *Chem. Rev.* **2009**, *109*, 2576–2589.
13. Humblot, V.; Barlow, S. M.; Raval, R. Two-Dimensional Organisational Chirality through Supramolecular Assembly of Molecules at Metal Surfaces. *Prog. Surf. Sci.* **2004**, *76*, 1–19.
14. Ernst, K. H. Supramolecular Surface Chirality. *Top. Curr. Chem.* **2006**, *265*, 209–252.
15. Spillmann, H.; Kiebele, A.; Stöhr, M.; Jung, T. A.; Bonifazi, D.; Cheng, F.; Diederich, F. A Two-Dimensional Porphyrin-Based Porous Network Featuring Communicating Cavities for the Templated Complexation of Fullerenes. *Adv. Mater.* **2006**, *18*, 275–279.
16. Matena, M.; Llanes-Pallas, A.; Enache, M.; Jung, T.; Wouters, J.; Champagne, B.; Stöhr, M.; Bonifazi, D. Conformation-Controlled Networking of H-Bonded Assemblies on Surfaces. *Chem. Commun.* **2009**, 3525–3527.
17. Pivetta, M.; Blüm, M.-C.; Patthey, F.; Schneider, W.-D. Two-Dimensional Tiling by Rubrene Molecules Self-Assembled in Supramolecular Pentagons, Hexagons, and Heptagons on a Au(111) Surface. *Angew. Chem., Int. Ed.* **2008**, *47*, 1076–1079.
18. Yokoyama, T.; Kamikado, T.; Yokoyama, S.; Mashiko, S. Conformation Selective Assembly of Carboxyphenyl Substituted Porphyrins on Au (111). *J. Chem. Phys.* **2004**, *121*, 11993–11997.
19. Fendt, L.; Stöhr, M.; Wintjes, N.; Enache, M.; Jung, T. A.; Diederich, F. Modification of Supramolecular Binding Motifs Induced by Substrate Registry: Formation of Self-Assembled Macrocycles and Chain-like Patterns. *Chem.—Eur. J.* **2009**, *15*, 11139–11150.
20. Heim, D.; Seufert, K.; Auwärter, W.; Aurisicchio, C.; Fabbro, C.; Bonifazi, D.; Barth, J. V. Surface-Assisted Assembly of Discrete Porphyrin-Based Cyclic Supramolecules. *Nano Lett.* **2010**, *10*, 122–128.
21. Heim, D.; Ecija, D.; Seufert, K.; Auwärter, W.; Aurisicchio, C.; Fabbro, C.; Bonifazi, D.; Barth, J. V. Self-Assembly of Flexible One-Dimensional Coordination Polymers on Metal Surfaces. *J. Am. Chem. Soc.* **2010**, *132*, 6783–6790.
22. Bombis, C.; Weigelt, S.; Knudsen, M. M.; Norgaard, M.; Busse, C.; Laegsgaard, E.; Besenbacher, F.; Gothelf, K. V.; Linderoth, T. R. Steering Organizational and Conformational Surface Chirality by Controlling Molecular Chemical Functionality. *ACS Nano* **2009**, *4*, 297–311.
23. Meunier, B. Metalloporphyrins as Versatile Catalysts for Oxidation Reactions and Oxidative DNA Cleavage. *Chem. Rev.* **1992**, *92*, 1411–1456.
24. Beletskaya, I.; Tyurin, V. S.; Tsivadze, A. Y.; Guilard, R.; Stern, C. Supramolecular Chemistry of Metalloporphyrins. *Chem. Rev.* **2009**, *109*, 1659–1713.
25. Forrest, S. R. Ultrathin Organic Films Grown by Organic Molecular Beam Deposition and Related Techniques. *Chem. Rev.* **1997**, *97*, 1793–1896.

26. Gust, D.; Moore, T. A.; Moore, A. L. Solar Fuels *via* Artificial Photosynthesis. *Acc. Chem. Res.* **2009**, *42*, 1890–1898.
27. Jung, T.; Schlittler, R.; Gimzewski, J. Conformational Identification of Individual Adsorbed Molecules with the STM. *Nature* **1997**, *386*, 696–698.
28. Yokoyama, T.; Yokoyama, S.; Kamidado, T.; Mashiko, S. Nonplanar Adsorption and Orientational Ordering of Porphyrin Molecules on Au(111). *J. Chem. Phys.* **2001**, *115*, 3814–3818.
29. Moresco, F.; Meyer, G.; Rieder, K.-H.; Ping, J.; Tang, H.; Joachim, C. TBPP Molecules on Copper Surfaces: A Low Temperature Scanning Tunneling Microscope Investigation. *Surf. Sci.* **2002**, *499*, 94–102.
30. Auwärter, W.; Weber-Bargioni, A.; Riemann, A.; Schiffrin, A.; Groning, O.; Fasel, R.; Barth, J. V. Self-Assembly and Conformation of Tetrapyridyl-Porphyrin Molecules on Ag(111). *J. Chem. Phys.* **2006**, *124* (19), 194708.
31. Auwärter, W.; Klappenberger, F.; Weber-Bargioni, A.; Schiffrin, A.; Strunskus, T.; Wöll, C.; Pennec, Y.; Riemann, A.; Barth, J. V. Conformational Adaptation and Selective Adatom Capturing of Tetrapyridyl-Porphyrin Molecules on a Copper (111) Surface. *J. Am. Chem. Soc.* **2007**, *129*, 11279–11285.
32. Weber-Bargioni, A.; Auwärter, W.; Klappenberger, F.; Reichert, J.; Lefrançois, S.; Strunskus, T.; Wöll, C.; Schiffrin, A.; Pennec, Y.; Barth, J. V. Visualizing the Frontier Orbitals of a Conformationally Adapted Metalloporphyrin. *ChemPhysChem* **2008**, *9*, 89–94.
33. Ecija, D.; Trelka, M.; Urban, C.; de Mendoza, P.; Mateo-Martín, E.; Rogero, C.; Martín-Gago, J. A.; Echavarren, A. M.; Otero, R.; Gallego, J. M.; Miranda, R. Molecular Conformation, Organizational Chirality, and Iron Metalation of *meso*-Tetramesitylporphyrins on Copper(100). *J. Phys. Chem. C* **2008**, *112*, 8988–8994.
34. Auwärter, W.; Seufert, K.; Klappenberger, F.; Reichert, J.; Weber-Bargioni, A.; Verdini, A.; Cvetko, D.; Dell'Angela, M.; Floreano, L.; Cossaro, A.; Bavdek, G.; Morgante, A.; Seitsonen, A. P.; Barth, J. V. Site-Specific Electronic and Geometric Interface Structure of Co-tetraphenyl-porphyrin Layers on Ag(111). *Phys. Rev. B* **2010**, *81*, 245403.
35. Kuhnle, A.; Linderoth, T. R.; Hammer, B.; Besenbacher, F. Chiral Recognition in Dimerization of Adsorbed Cysteine Observed by Scanning Tunnelling Microscopy. *Nature* **2002**, *415*, 891–893.
36. Weigelt, S.; Busse, C.; Petersen, L.; Rauls, E.; Hammer, B.; Gothelf, K. V.; Besenbacher, F.; Linderoth, T. R. Chiral Switching by Spontaneous Conformational Change in Adsorbed Organic Molecules. *Nat. Mater.* **2006**, *5*, 112–117.
37. Klappenberger, F.; Kühne, D.; Krenner, W.; Silanes, I.; Arnau, A.; García de Abajo, F. J.; Klyatskaya, S.; Ruben, M.; Barth, J. V. Dichotomous Array of Chiral Quantum Corrals by a Self-Assembled Nanoporous Kagomé Network. *Nano Lett.* **2009**, *9*, 3509–3514.
38. Lobo-Checa, J.; Matena, M.; Muller, K.; Dil, J. H.; Meier, F.; Gade, L. H.; Jung, T. A.; Stohr, M. Band Formation from Coupled Quantum Dots Formed by a Nanoporous Network on a Copper Surface. *Science* **2009**, *325*, 300–303.
39. Pennec, Y.; Auwärter, W.; Schiffrin, A.; Weber-Bargioni, A.; Riemann, A.; Barth, J. V. Supramolecular Gratings for Tuneable Confinement of Electrons on Metal Surfaces. *Nat. Nanotechnol.* **2007**, *2*, 99–103.
40. Schiffrin, A.; Reichert, J.; Auwärter, W.; Jahnz, G.; Pennec, Y.; Weber-Bargioni, A.; Stepanyuk, V. S.; Niebergall, L.; Bruno, P.; Barth, J. V. Self-Aligning Atomic Strings in Surface-Supported Biomolecular Gratings. *Phys. Rev. B* **2008**, *78*, 035424.
41. Theobald, J. A.; Oxtoby, N. S.; Phillips, M. A.; Champness, N. R.; Beton, P. H. Controlling Molecular Deposition and Layer Structure with Supramolecular Surface Assemblies. *Nature* **2003**, *424*, 1029–1031.
42. Stepanow, S.; Lingenfelder, M.; Dmitriev, A.; Spillmann, H.; Delvigne, E.; Lin, N.; Deng, X.; Cai, C.; Barth, J. V.; Kern, K. Steering Molecular Organization and Host−Guest Interactions Using Tailor-Made Two-Dimensional Nanoporous Coordination Systems. *Nat. Mater.* **2004**, *3*, 229–233.
43. Kibele, A.; Bonifazi, D.; Cheng, F.; Stöhr, M.; Diederich, F.; Jung, T.; Spillmann, H. Adsorption and Dynamics of Long-Range Interacting Fullerenes in a Flexible, Two-Dimensional, Nanoporous Porphyrin Network. *ChemPhysChem* **2006**, *7*, 1462–1470.
44. Stepanow, S.; Lin, N.; Barth, J. V.; Kern, K. Binding of Organic Guests at Two-Dimensional Metallosupramolecular Hosts. *Chem. Commun.* **2006**, 2153–2155.
45. Wintjes, N.; Bonifazi, D.; Cheng, F.; Kibele, A.; Stöhr, M.; Jung, T.; Spillmann, H.; Diederich, F. A Supramolecular Multiposition Rotary Device. *Angew. Chem., Int. Ed.* **2007**, *46*, 4089–4092.
46. Bonifazi, D.; Mohnani, S.; Llanes-Pallas, A. Supramolecular Chemistry at the Interfaces: Molecular Recognition on Nanopatterned Surfaces. *Chem.—Eur. J.* **2009**, *15*, 7004–7025.
47. MacLeod, J. M.; Ivasenko, O.; Fu, C.; Taerum, T.; Rosei, F.; Perepichka, D. F. Supramolecular Ordering in Oligothiophene-Fullerene Monolayers. *J. Am. Chem. Soc.* **2009**, *131*, 16844–16850.
48. Piot, L.; Silly, F.; Tortech, L.; Nicolas, Y.; Blanchard, P.; Roncali, J.; Fichou, D. Long-Range Alignments of Single Fullerenes by Site-Selective Inclusion into a Double-Cavity 2D Open Network. *J. Am. Chem. Soc.* **2009**, *131*, 12864–12865.
49. Auwärter, W.; Schiffrin, A.; Weber-Bargioni, A.; Pennec, Y.; Riemman, A.; Barth, J. Molecular Nanoscience and Engineering on Surfaces. *Int. J. Nanotechnol.* **2008**, *5*, 1171–1193.
50. Createc D-74391 Erligheim, Germany.
51. *HYPERCHEM*; Gainesville, FL.
52. Horcas, I.; Fernández, R.; Rodríguez, J. M.; Colchero, J.; Gómez-Herrero, J.; Baró, A. M. WSxM: A Software for Scanning Probe Microscopy and a Tool for Nanotechnology. *Rev. Sci. Instrum.* **2007**, *78*, 013705.